

University of New England

DUNE: DigitalUNE

Pharmaceutical Sciences Faculty Publications

Pharmaceutical Sciences Faculty Works

2-2-2017

Transcriptomes Reflect The Phenotypes Of Undifferentiated, Granulocyte And Macrophage Forms Of HL-60/S4 Cells

David B. Mark Welch

Anna Jauch

Jörg Langowski

Ada L. Olins

Donald E. Olins

Follow this and additional works at: https://dune.une.edu/pharmsci_facpubs



Part of the [Pharmacy and Pharmaceutical Sciences Commons](#)



Transcriptomes reflect the phenotypes of undifferentiated, granulocyte and macrophage forms of HL-60/S4 cells

David B. Mark Welch, Anna Jauch, Jörg Langowski, Ada L. Olins & Donald E. Olins

To cite this article: David B. Mark Welch, Anna Jauch, Jörg Langowski, Ada L. Olins & Donald E. Olins (2017) Transcriptomes reflect the phenotypes of undifferentiated, granulocyte and macrophage forms of HL-60/S4 cells, *Nucleus*, 8:2, 222-237, DOI: [10.1080/19491034.2017.1285989](https://doi.org/10.1080/19491034.2017.1285989)

To link to this article: <https://doi.org/10.1080/19491034.2017.1285989>



© 2017 Taylor & Francis



[View supplementary material](#)



Accepted author version posted online: 02 Feb 2017.
Published online: 13 Apr 2017.



[Submit your article to this journal](#)



Article views: 628



[View related articles](#)

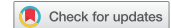


[View Crossmark data](#)



Citing articles: 5 [View citing articles](#)

ORIGINAL RESEARCH



Transcriptomes reflect the phenotypes of undifferentiated, granulocyte and macrophage forms of HL-60/S4 cells

David B. Mark Welch^a, Anna Jauch^b, Jörg Langowski^c, Ada L. Olins^d, and Donald E. Olins^d

^aJosephine Bay Paul Center for Comparative Molecular Biology and Evolution, Marine Biological Laboratory, Woods Hole, MA, USA; ^bInstitute of Human Genetics, University of Heidelberg, Heidelberg, Germany; ^cDivision Biophysics of Macromolecules, B040, German Cancer Research Center (DKFZ), TP3, Heidelberg, Germany; ^dUniversity of New England, College of Pharmacy, Department of Pharmaceutical Sciences, Portland, ME, USA

ABSTRACT

To understand the chromatin changes underlying differential gene expression during induced differentiation of human leukemic HL-60/S4 cells, we conducted RNA-Seq analysis on quadruplicate cultures of undifferentiated, granulocytic- and macrophage-differentiated cell forms. More than half of mapped genes exhibited altered transcript levels in the differentiated cell forms. In general, more genes showed increased mRNA levels in the granulocytic form and in the macrophage form, than showed decreased levels. The majority of Kyoto Encyclopedia of Genes and Genomes (KEGG) pathways were significantly enriched in genes that exhibited differential transcript levels after either RA or TPA treatment. Changes in transcript levels for groups of genes with characteristic protein phenotypes, such as genes encoding cytoplasmic granular proteins, nuclear envelope and cytoskeletal proteins, cell adhesion proteins, and proteins involved in the cell cycle and apoptosis illustrate the profound differences among the various cell states. In addition to the transcriptome analyses, companion karyotyping by M-FISH of undifferentiated HL-60/S4 cells revealed a plethora of chromosome alterations, compared with normal human cells. The present mRNA profiling provides important information related to nuclear shape changes (e.g., granulocyte lobulation), deformability of the nuclear envelope and linkage between the nuclear envelope and cytoskeleton during induced myeloid chromatin differentiation.

ARTICLE HISTORY

Received 6 December 2016

Revised 2 January 2017

Accepted 18 January 2017

KEYWORDS

Acute myeloid leukemia; apoptosis; cell attachment; cell differentiation; cell division; cytoskeleton; granulocyte; karyotype; macrophage; mRNA levels; nuclear envelope

Introduction

The human myeloid leukemia cell line (HL-60) was originally isolated from a female patient with presumed acute promyelocytic leukemia (APL).^{1,2} These cells can be differentiated *in vitro* from a rapidly growing promyelocytic form to a nongrowing form, resembling neutrophils with segmented (lobulated) nuclei, by adding dimethyl sulfoxide (DMSO) to the growth medium.² A similar, but more complete, differentiation toward neutrophil form can be achieved by the addition of retinoic acid (RA).³ Eleven years after the discovery of HL-60, it was reclassified as an acute myeloblastic leukemia (AML) with maturation, due to the absence of the APL characteristic t(15:17) chromosome translocation.⁴ Shortly after the initial isolation of HL-60 cells, it was discovered that treating the undifferentiated cells with phorbol ester (TPA) led to

rapid cessation of cell division and attachment of the treated cells to culture dishes, exhibiting characteristics of macrophage.^{5,6} Other investigators also described the differentiation of HL-60 cells into monocytic form following exposure to vitamin D3.^{7,8} These initial studies, demonstrating the multipotential character of HL-60 cells to differentiate along various myeloid directions, were summarized in an early review by one of the original discoverers of this important cell line.⁹

A number of studies have analyzed transcript levels in the HL-60 cell system, comparing undifferentiated and differentiated cell forms. An early study examined the mRNA level of the neutrophil primary granule protein myeloperoxidase; using *in vivo* radiolabeling and Northern blot analysis.¹⁰ The transcript level was

CONTACT Donald E. Olins  aolins@une.edu, dolins@une.edu  University of New England, College of Pharmacy, Department of Pharmaceutical Sciences, 716 Stevens Avenue, Portland, ME, USA.

Color versions of one or more of the figures in the article can be found online at www.tandfonline.com/kncl.

 Supplemental data for this article can be accessed on the [publisher's website](http://www.tandfonline.com/kncl).

reduced by addition of TPA. Microarray analyses of transcription in HL-60 cells examined granulocytic differentiation induced by RA¹¹ or DMSO,¹² macrophage differentiation induced by TPA,¹³ transcript changes induced by vitamin D3¹⁴ and a comparison of transcript level changes induced by RA or by vitamin D3.¹⁵ More recently, transcription in HL-60 and 2 other undifferentiated myeloid leukemia cell lines, K562 and THP1, were compared by RNA-Seq and examination of enriched KEGG pathways.¹⁶ However, this analysis did not include differentiated cell forms.

The subline HL-60/S4 was developed in 1992, and exhibits several characteristics that discriminate it from the parent line, including faster differentiation.¹⁷ For instance, this rapidly responding cell line develops nuclear segmentation in 4 d; whereas the parent HL-60 line requires at least 6 d for the same level of differentiation.¹⁸ In addition, karyotype differences are documented later in the present study. Our laboratory has published extensively on HL-60/S4 in an investigation of nuclear shape, chromatin structure and cytoskeletal changes during differentiation induced by RA, TPA and vitamin D3 (e.g.,¹⁹⁻²⁵). In our hands, HL-60/S4 cells have proven to be robust and to yield highly reproducible cell differentiation. Furthermore, HL-60/S4 has now become available for purchase from ATCC. Defining the mRNA levels resulting from the differentiation of HL-60/S4 by RA and TPA is central to interpreting the functional significance of observed changes in nuclear architecture and chromatin structure.

In the present study, we determined mRNA levels in untreated HL-60/S4 cells and in cells treated separately with RA and TPA, using quadruplicate independent samples. Many KEGG pathways were enriched after one or both treatments, and we discuss illustrative groups of gene transcripts that relate to the observed phenotypic characteristics of the differentiated HL-60/S4 cells. The comprehensive data from this model cell system furnishes transcript level constraints that must, in part, reflect myeloid chromatin structural changes.

Results

Due to the large amount of data generated by RNA-Seq, we concentrated upon quadruplicates of only 3 cell states: undifferentiated asynchronous HL-60/S4 cells, and RA- and TPA-treated differentiated cells,

both collected after 4 d of treatment. We measured mRNA levels of all transcripts annotated in the UCSC hg19 (NCBI GRCh37) human reference genome with RSEM,²⁶ which uses a maximum likelihood expectation-maximization algorithm to estimate the transcript abundance of individual isoforms. The hg19 does not include ribosomal rRNA genes or the mitochondrial genome. Paired-end RNA-Seq reads from each library of the 3 experimental conditions mapped to ~30,000 isoforms, representing ~16,000 genes with unique Human Genome Nomenclature Committee (HGNC) identifiers (Table 1). We determined which isoforms were differentially expressed with EBSeq,²⁷ which uses an empirical Bayesian approach to model variance among replicates and between experimental conditions to determine the posterior probability of differential transcript abundance (or “expression,” PPDE) for each isoform between all comparisons of experimental conditions. Because the variances of all isoforms are modeled together the false discovery rate (FDR) for any isoform is 1 – PPDE. Low variance across biologic replicates and deep sequencing led to PPDE < 0.05 for some isoforms even when the fold-change was low (< 2); in contrast, for isoforms with low expression across conditions the PPDE could be > 0.05, even when fold-change was high. Both treat-

Table 1. Summary of significant differences in gene transcript levels, comparing the differentiated states of HL-60/S4 cells.

	Isoforms / Genes RA	TPA
Mapped	29,838 / 16,189	30,485 / 16,526
Decreased transcripts	5,045 / 3,900	6,336 / 4,528
Increased transcripts	5,937 / 4,249	7,505 / 5,156
Decreased transcripts in both treatments	3,516 / 2,785	3,516 / 2,785
Decreased more in one, than in the other treatment	1,171 / 1,022	386 / 361
Increased transcripts in both treatments	3,920 / 2,937	3,920 / 2,937
Increased more in one, than in the other treatment	712 / 594	1,630 / 1,361
Increased transcripts in one, with decreased transcripts in the other treatment	221 / 195	412 / 362
	Enriched KEGG Pathways	
Increased isoform transcripts	137	143
Decreased isoform transcripts	106	80
Increased transcripts in both treatments	126	126
Decreased transcripts in both treatments	65	65

Table 1. There are 46,923 isoforms, defined by unique refseq identifiers, and 25,370 genes, defined by unique HGNC names, annotated in our hg19 reference genome. Reads from the control HL-60/S4 cells mapped to 29,753 isoforms and 15,998 genes. We required isoforms to have an RSEM estimated transcript level of at least 1 to be considered mapped, and to have an EBSeq posterior probability of differential transcript level of at least 0.95.

ments caused widespread changes in mRNA transcript levels (Table 1). In general, more genes increased than decreased transcript levels after treatment, and more genes were affected by TPA treatment than by RA treatment. When a gene showed increased transcript levels after either treatment, it was likely to have significantly higher levels after TPA. When a gene showed decreased transcript levels after either treatment, it was likely to have significantly lower levels after RA. More than half of 315 Kyoto Encyclopedia of Genes and Genomes (KEGG) pathways were significantly enriched in genes with PPDE < 0.05 after either treatment. We, therefore, limited our analyses to sets of genes and KEGG pathways likely to play a direct role in the morphological and biochemical changes associated with HL-60/S4 differentiation into granulocyte and macrophage forms, some of which we have previously studied. Examples of these gene groups with related phenotypic effects are presented below.

Cytoplasmic granule proteins

An emblematic feature of blood neutrophils is the profusion of cytoplasmic granules, collectively containing about 300 different proteins.^{28,29} Traditionally, these granules have been regarded as being packaged with potent antibacterial enzymes and peptides. It is now clear that the collection of proteins encompasses other functions as well (e.g., facilitating the adhesion of monocytes to the endothelium), being packaged into 3 classes of granules (1°, 2°, 3°).

We examined the expression of genes encoding 14 of the principal granule proteins. Compared to untreated HL-60/S4 controls, 10 genes had significantly different transcript levels in RA-treated cells and 13 had significantly different levels in TPA-treated cells (Fig. 1 and Supplemental Table 1). With the exception of cystatin 3 (CST3), all of the genes also had significantly different transcript levels between RA and TPA treated cells. Transcripts for defensins (DEFA1, 3 and 4) increased in RA-treated cells and decreased in TPA-treated cells. Transcripts for alkaline phosphatase (ALPL) increased, while cathepsin G (CTSG) and myeloperoxidase (MPO) decreased in TPA-treated cells. RA treatment did not significantly change the transcript levels for any of these 3 genes. In other cases, such as the bactericidal/permeability-increasing protein BPI, cytostatin F (CST7), cathepsin D (CTSD), and elastase (ELANE), the direction of the transcriptional response was the same after the 2 treatments, but the magnitude of the response differed. Our results with HL-60/S4, compared with a previous examination of the effects of RA and TPA on the parental HL-60 cell line using Northern blot assays, concur on decreased mRNA levels of MPO after TPA treatment,¹⁰ but disagree with published results which show a decrease in MPO mRNA levels after RA treatment.^{10,30} This may represent a difference in gene regulation and/or MPO mRNA stability, comparing the parent and derived cell lines. In other studies of HL-60 cells, expression microarrays showed increased levels of defensins and cathepsin D after RA treatment,¹¹ implying that for

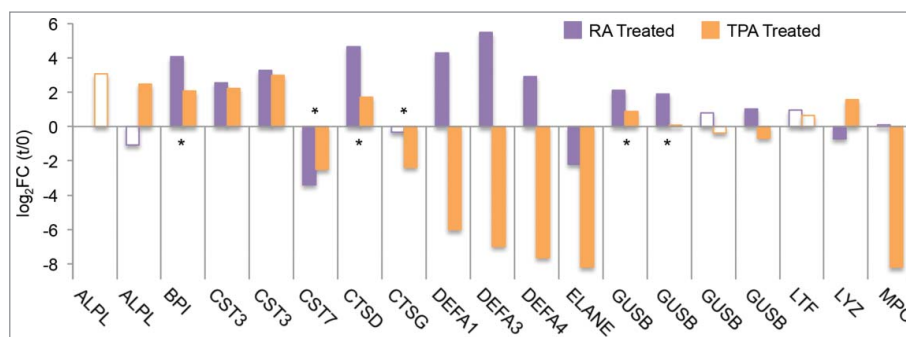


Figure 1. Differential transcript levels for cytoplasmic granular proteins. Bars indicate the ratio of RSEM (RNA-Seq by Expectation-Maximization) expected counts of treatment (RA or TPA) compared with control (undifferentiated HL-60/S4 cells). Gene names are HUGO Gene Nomenclature Committee (HGNC) gene symbols; repetition of the gene name indicates multiple isoforms of the gene. Bars indicate difference in transcript levels from untreated control: solid bars indicate differential transcript levels with posterior probability ≥ 0.95 ; open bars indicate posterior probability < 0.95. Asterisks indicate that the transcript level after one treatment is significantly different than the other treatment (p.p. ≥ 0.95), when both exhibit increased or decreased transcript levels. Only isoforms where the total RSEM expected count was ≥ 10 across all 3 cell states, or where the contribution of the isoform to the total count of the gene was ≥ 0.05 for at least one condition, are shown. Details for all isoforms, including NCBI refseq identifiers, are in Supplemental Table 1.

these genes, both the parent and derived cell lines respond in a similar fashion to RA-induced differentiation, generating a similar granule protein repertoire. The major conclusion of this section is that there is a significant difference in granule protein transcript levels comparing RA and TPA treated HL-60/S4 cells. Furthermore, the decreased transcripts of DEFA and MPO genes, following TPA treatment of HL-60/S4 cells, suggests that the TPA-induced macrophage are less committed to destroying bacteria than are the RA-induced granulocytes.

Nuclear envelope and cytoskeletal proteins

Many of our previous studies on HL-60/S4 have been concerned with 2 related questions: 1) What changes within the nuclear envelope and in the cytoskeleton, following RA treatment, affect nuclear shape and cell deformability? 2) Are these changes different from those in TPA treated cells (which do not show nuclear segmentation)? Our earlier studies on the first question, using immunostaining and immunoblotting, demonstrated the presence of elevated levels of lamin B receptor (LBR) and a reduction in levels of lamin A (LMNA) in the nuclear envelope of RA treated HL-60/S4 cells. We speculated that these changes in protein level caused nuclear lobulation and deformability of the granulocytic nuclei.^{19-24,31,32}

As can be seen in Fig. 2 and Supplemental Table 2, there is a dramatic difference in transcript level of

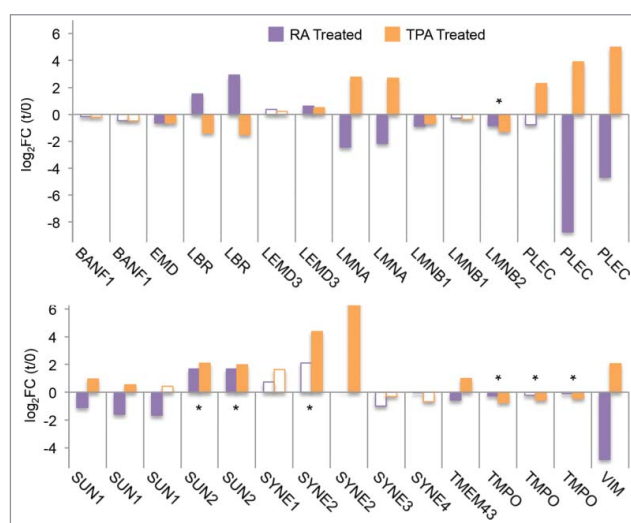


Figure 2. Differential transcript levels for nuclear envelope and cytoskeletal proteins. Graphical representation is the same as described in the legend for Fig. 1. Details for all isoforms, including NCBI refseq identifiers, are in Supplemental Table 2.

LMNA between the 2 differentiated cell forms, with significant decrease following RA, versus a significant increase following TPA. Somewhat surprisingly, transcript levels of lamin B1 (LMNB1) and lamin B2 (LMNB2) decreased after both treatments. Our earlier immunoblotting studies of nuclear envelope proteins²² had not detected reductions in LMNB1 and LMNB2, compared with undifferentiated cells. It is, of course, possible that the reduction in LMNB1 and LMNB2 transcript levels is compensated by increased stability of the lamin B proteins; whereas, the decrease in LMNA transcripts is more accurately reflected in the protein level.

Likewise, there are significant differences between the 3 cell states in the transcription levels of non-lamin inner nuclear membrane (INM) proteins, which “bridge” directly or indirectly between the INM and underlying heterochromatin. Lamin B receptor (LBR) mRNA is elevated following RA treatment and reduced after TPA, agreeing with earlier immunostaining and immunoblotting experiments.²² Emerin (EMD) mRNA is reduced after either treatment, also in agreement with earlier immunochemical studies.²² However, only after TPA treatment is emerin present in the INM, due in part to the requirement for lamin A as a binding partner. In the absence of lamin A, emerin is found within the cytoplasm.²¹ Transcripts of lamina-associated polypeptide 2 (a.k.a thymopoietin or TMPO) are reduced after both treatments, and significantly more so after treatment with TPA. This observation does not agree with earlier immunoblotting data,²² which may indicate that the protein is very stable. Transcript levels of another INM protein gene, LEMD3, modestly but significantly increase after either treatment.

Within the INM, the SUN proteins primarily function by connecting to KASH-domain proteins of the outer nuclear envelope, which in turn connect to the cytoskeleton, constituting the “linker of nucleoskeleton and cytoskeleton,” or LINC complex.^{33,34} In our transcriptome data, the SUN1 transcript level is decreased in RA treated cells and increased in TPA treated cells, while the SUN2 transcript is elevated after either treatment (although, more so after TPA). Both of these observations are in good agreement with our earlier immunochemical data.²² The transcript level for the KASH-domain protein nesprin 2 (SYNE2), which binds to the actin cytoskeleton, is increased after TPA treatment. There is also a weak

indication of an increased level of the nesprin 1 (SYNE1) transcript. Our previous immunochemical study²² indicated that nesprin 1 protein was elevated and nesprin 2 was not detectable. Without additional information about mRNA and protein turnover, this particular conundrum must remain. Even so, the greater amount of the LINC complex proteins in the macrophage cell form (TPA) of HL-60/S4, compared with the granulocytic form (RA), seems largely supported by the present transcript data.

Finally, the mRNA encoding the cytoskeleton protein vimentin (VIM) is significantly decreased in RA treated and increased in TPA treated cells (similar to lamin A, Fig. 2). Multiple isoforms of plectin (PLEC), some of which connect with vimentin, show the same pattern. It is possible that the multiple variants of plectin observed in the transcriptome may correlate with the multiple immunoblot bands of plectin described previously.²² In summary, the transcriptomes of the RA and TPA treated HL-60/S4 cells support the conception that the granulocytic forms possess a more malleable nuclear envelope and cytoskeleton than within macrophage forms, consistent with their normal counterpart cell functions.

Cell cycle

After RA addition to HL-60 cells (day 0), there is an increase of “doubling time,” beginning at ~day 2 and achieving a growth plateau by ~day 4.³ In contrast, the addition of TPA to HL-60 cells results in an almost immediate cessation of cell doubling.^{5, 6} We have observed similar differences in cell cycling behavior at day 4 in the HL-60/S4 subline. The % of cells in S phase declines with differentiation; 0, RA and TPA cells exhibit 23.5, 12.9 and 5.7% cells in S, respectively. In parallel, more cells reside in G1 phase; 0, RA and TPA cells exhibit 48.6, 64.9 and 70.6% in G1, respectively. G2 phase remains relatively unchanged at ~20% of the cell cycle. In an effort to understand the underlying mechanism for this large difference in cell cycle behavior, we examined the steady-state mRNA levels of the cyclins (CNN) and their partner cyclin-dependent kinases (CDK). These proteins, and CDK inhibitors, are well known to affect cell cycle progression^{35,36} (Fig. 3 and Supplemental Table 3).

Fig. 3a shows the change in transcript levels of cyclins A-H after treatment with RA or TPA. Cyclin A1 (CCNA1) isoform transcripts are reduced in RA treated,

but significantly increased in TPA treated cells. Cyclin A1 protein is generally confined to the normal testis and is regarded as involved in meiosis, but has been recently described in AML cells.³⁷ Among other cyclins, there is a decreased transcript level of E1 after both treatments, while levels of A2, B1, B2, D2, E2 and F are decreased after treatment with TPA but not RA; transcript levels of D1 and D3 are increased after both. CDK2, 4, 6, and 7 transcript levels are reduced after both treatments. In addition, CDK1 mRNA is reduced after TPA (Fig. 3b). Overall, this pattern of changes in transcript abundance suggests that TPA treatment leads to reduction in the protein complexes CDK1/CCNB1 (involved in early events of mitosis, including chromosome condensation and NE breakdown), CDK2/CCNE1 (required for the G1 to S transition) and CDK2/CCNA2 (required for progress through S). One other important finding is that the mRNA levels for p21 (CDN1A, an inhibitor of CDK2 and CDK4/cyclin complexes), p16 (CDN2A, an inhibitor of CDK4/CCND and CDK6/CCDN complexes) and p15 (CDN2B, an inhibitor of CDK4 and CDK6 complexes) are significantly increased after TPA, more so than after RA treatment (Fig. 3c). The increase in p21 in TPA treated HL-60 cells was earlier observed by immunoblotting.³⁸ In summary, it appears that the more rapid cessation of cell division seen with TPA treated cells, compared with RA treated cells, may result from a faster reduction of CDK and cyclin transcripts and a significant inhibition of the protein complexes needed for cell cycle progression.

An additional issue pertains to histone H1 phosphorylation/dephosphorylation. We previously reported that when HL-60/S4 is differentiated using RA or TPA, the H1 subtypes (H1.2, H1.4 and H1.5) are extensively dephosphorylated without significant changes in protein levels²¹ The effects are more profound with TPA than with RA treatment. The current view is that H1 phosphorylation at serine/threonine sites is accomplished primarily by CDK2,³⁹ which we have demonstrated has much reduced transcript levels after RA and TPA (Fig. 3b).

Apoptosis

Granulocytic differentiated forms of HL-60 die by apoptosis.⁴⁰ Death begins around day 6 after RA treatment, with increases in caspases 1 and 3 on day 2, as revealed by immunoblotting and Northern blots,⁴¹ and a loss of anti-apoptotic BCL2 by day 7. The

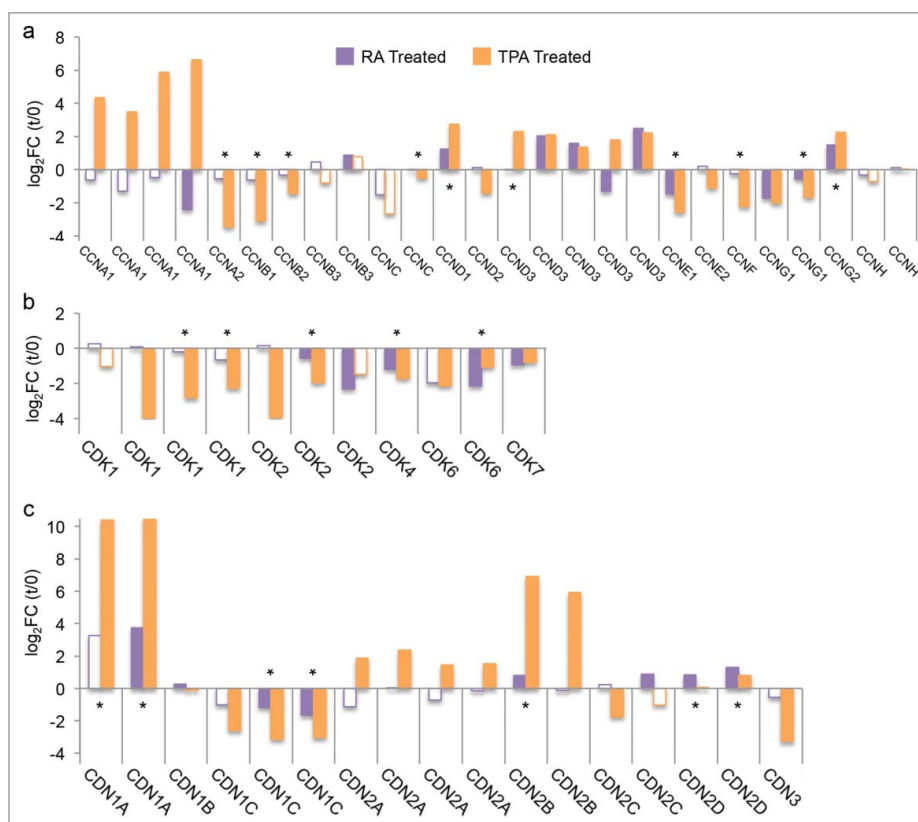


Figure 3. Differential transcript levels for proteins involved in the cell cycle. (A) Cyclins; (B) Cyclin Dependent Kinases; (C) CDK Inhibitors. Graphical representation is the same as described in the legend for Fig. 1. Details for all isoforms, including NCBI refseq identifiers, are in Supplemental Table 3.

mechanism of cell death in TPA treated HL-60 cells is somewhat more complex.^{38,42} These studies demonstrated that a small fraction (~10%) of the HL-60 cells do not differentiate after the addition of TPA, do not attach and do undergo apoptosis. The attached cells, which are overwhelmingly stopped in G1 phase, remain alive. Gradually, cells detach and exhibit apoptosis. It has been demonstrated that focal adhesion kinase (FAK) shows increased transcripts following TPA treatment and possesses an anti-apoptotic function.⁴³ The present TPA treated HL-60/S4 transcriptome data set was obtained from attached cells at day 4. The free-floating cell fraction with obvious apoptosis was removed by decanting the tissue culture medium, before RNA purification.

To determine if differences in the processes of cell death between RA and TPA treated HL-60/S4 cells are correlated with genetic mechanisms of apoptosis, we examined changes in transcript levels of caspases and other genes involved in apoptosis (Fig. 4 and Supplemental Table 4). Consistent with Northern blot results,⁴¹ we observe a significant increase in mRNAs

for multiple isoforms of caspase 1 (CASP1) and a significant decrease in both isoforms of BCL2 in RA treated cells. RA treated cells also have increased transcripts for initiator caspases 8, 9, and 10 and of effector caspase 7 (an increased mRNA level of CASP3 observed at day 2 is not evident in these samples, which are from day 4). Besides sufficient and suitable caspases, RA treated cells should be able to utilize an extrinsic “Cell Death Receptor” pathway, due to elevated mRNAs of the death receptor tumor necrosis factor receptor (TNFRSF1A) and associated proteins TRADD and TRAF1, which leads to activation of CASP9 or 10. Transcripts of TRAF2, which interacts with TRADD and TRAF1 to inhibit caspase activity, are reduced following RA or TPA treatment. However, the slight reduction of TNFRSF1A following TPA, may be enough to reduce apoptosis by “muting” the consequence of dramatically increased levels of TRAF1 transcript. It is also conceivable that the intrinsic mitochondrial pathway can initiate apoptosis in RA treated cells. There is increased mRNA of “apoptotic protease activating factor 1” (APAF1), which

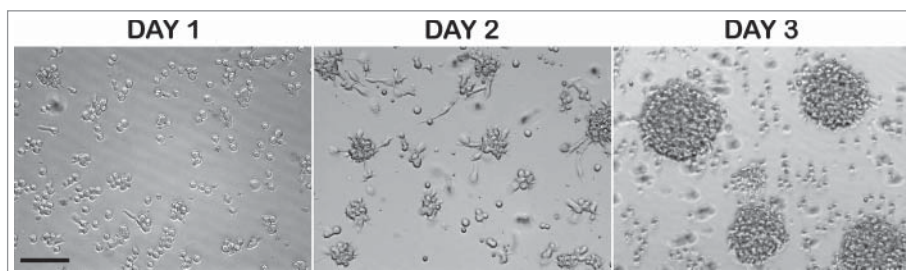


Figure 5. Light microscopic images of HL-60/S4 cells following treatment with 16 nM TPA. Cell attachment and progressive cell clustering are readily apparent. “Day,” refers to the days after addition of TPA. Magnification bar, 100 μ m.

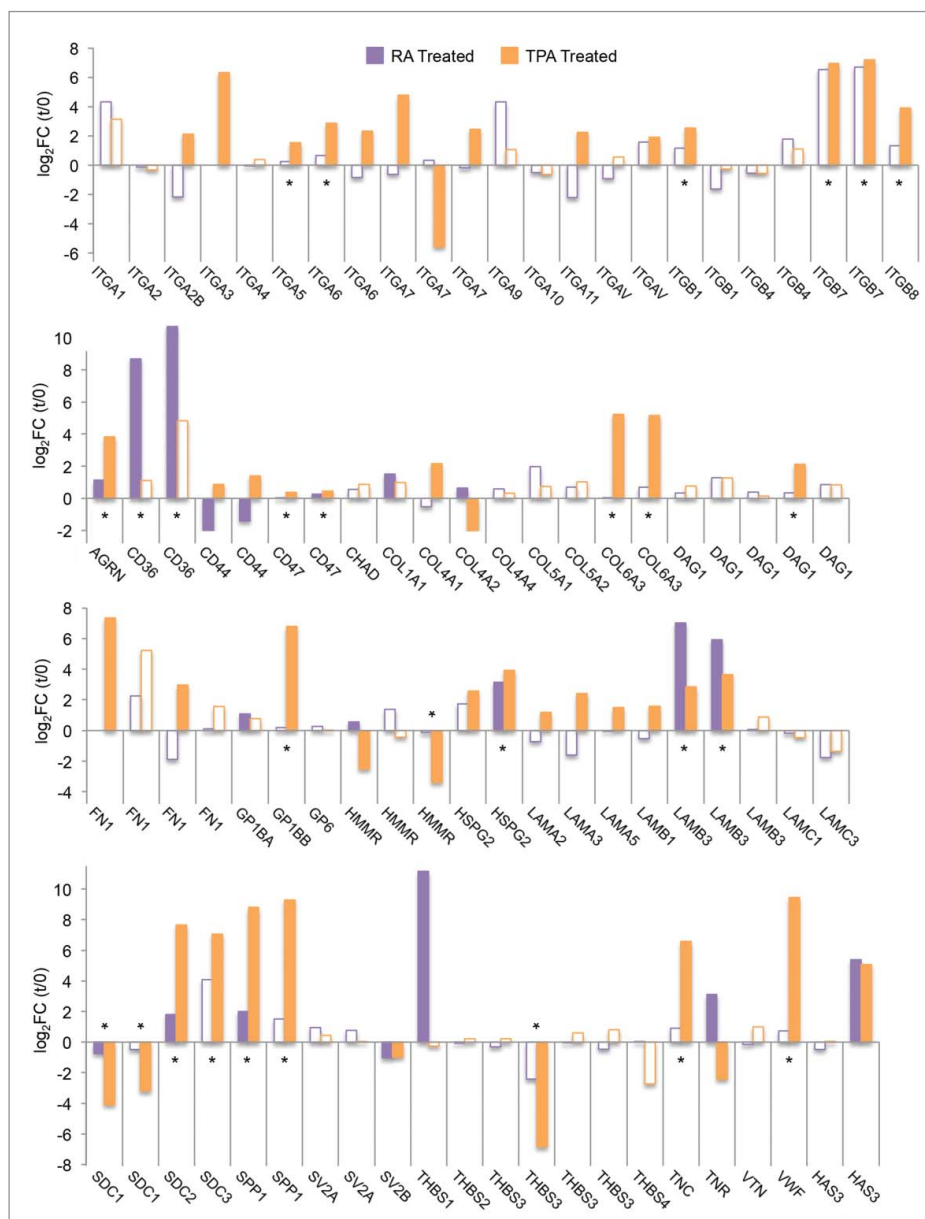


Figure 6. Differential transcript levels for proteins involved in cell attachment. KEGG Pathway: “Extracellular Matrix (ECM) Receptor Interactions.” Graphical representation is the same as described in the legend for Fig. 1. Details for all isoforms, including NCBI refseq identifiers, are in Supplemental Table 5.

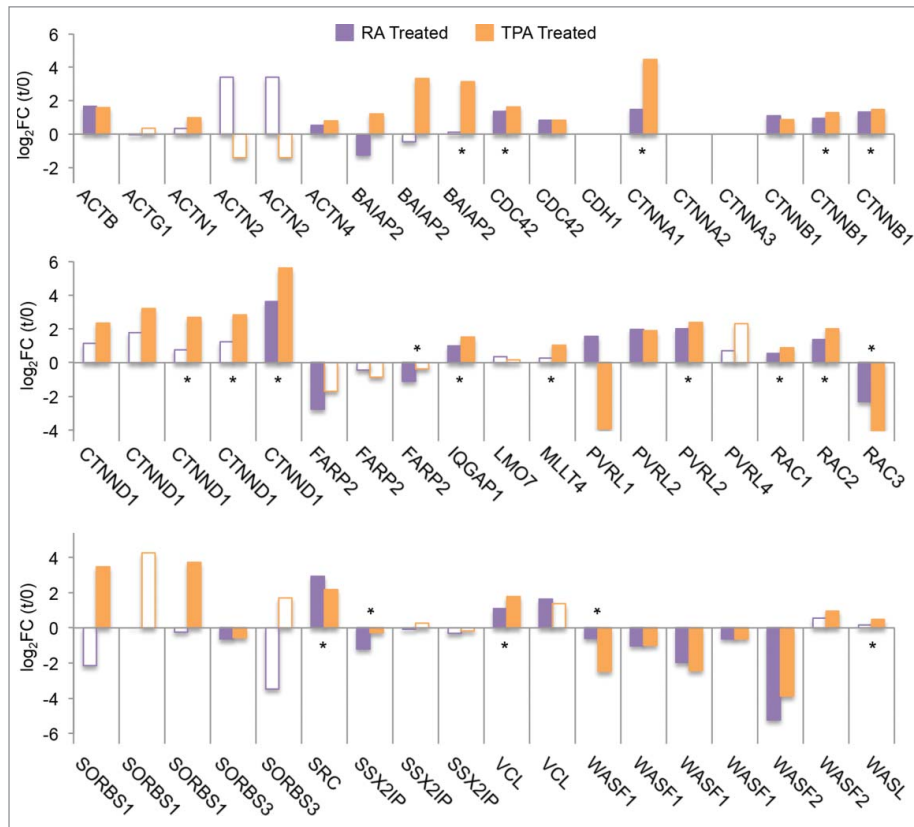


Figure 7. Differential transcript levels for proteins involved in cell attachment. KEGG Pathways: “Adherens Junctions” and “Cell Adhesion Molecules.” Graphical representation is the same as described in the legend for Fig. 1. Details for all isoforms, including NCBI refseq identifiers, are in Supplemental Table 5.

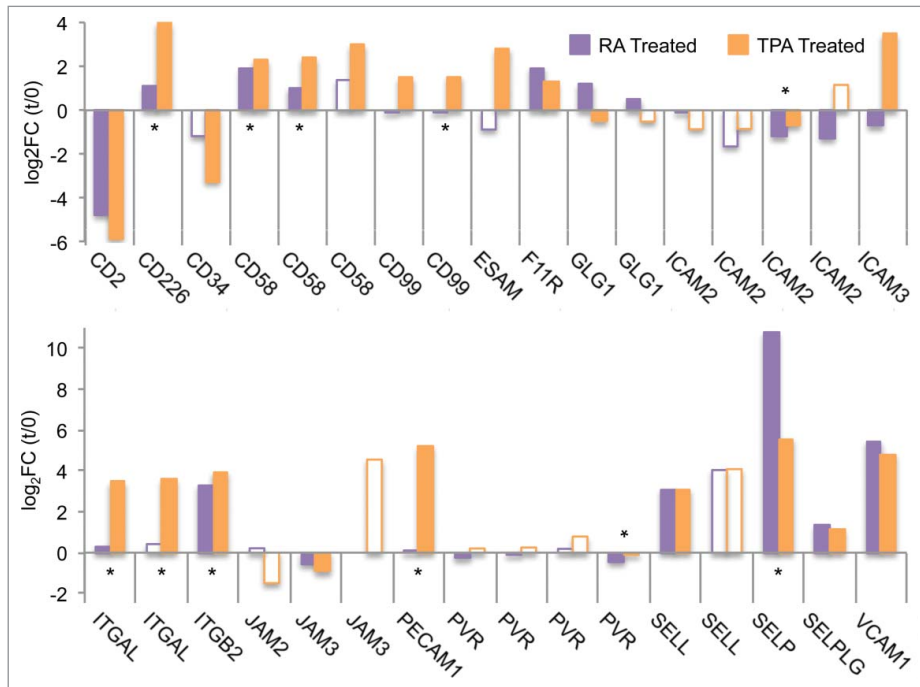


Figure 8. Differential transcript levels for proteins involved in cell attachment. KEGG Pathway: “Leukocyte Transendothelial Migration.” Graphical representation is the same as described in the legend for Fig. 1. Details for all isoforms, including NCBI refseq identifiers, are in Supplemental Table 5.

fibronectin (FN1), laminins (LAMA2, 3, 5, LAMB1), ostopontin (SPP1), perlecan (HSPG2), tenascin (TCN), and von Willebrand Factor (VWF), and for genes encoding many integrins (ITGA2B, A3, A5, A6, A7, A11, B1, B7, B8). Among cell-surface glycoproteins, CD44 has increased transcript levels following TPA treatment and decreased levels following RA treatment. Among the few genes with increased transcripts in RA treated cells (and not in TPA-treated cells) are the receptor CD36 and its ligand thrombospondin (THBS1). We do not know what factors are critical for defining the difference in attachment behavior after TPA and RA treatment, but the increased mRNAs for multiple ECMs and integrins after TPA treatment, contrasted with the more limited RA-specific gene transcripts (i.e., CD36 and THBS1), may be of importance.

The basis for cell clustering after TPA treatment is even more mysterious. One possibility is the establishment of adherens junctions and cell adhesion molecules (Fig. 7). Cadherin 1 (CDH1), responsible for Ca^{2+} dependent cell adhesion, reveals minimal transcripts in HL60/S4 cells under either control or treatment conditions. However, mRNAs of genes making up the complete pathway for Ca^{2+} independent adherens junctions, including nectin 2 (PVRL2), afadin (MLLT4), α , β , and delta catenins (CTTN1, B1, D1) and actins (ACTN, ACTB, ACTG1) clearly increase after treatment with TPA. Some, but not all, of these genes increase their transcript levels after RA treatment, but their steady-state levels after TPA treatment are consistently significantly higher.

A second possibility is that clustering is a product of activation of the leukocyte transendothelial migration pathway (Fig. 8). Many genes in this KEGG pathway reveal increased transcripts after both RA and TPA treatment. Intriguingly, CD226, which binds nectin 2, has higher transcript levels after TPA than after RA treatment. Transcript levels for the genes encoding the endothelial cell adhesion molecules PECAM1 and ESAM are increased after TPA, but not after RA treatment. ESAM is implicated in forming endothelial tight junctions rather than leukocyte migration, but other genes specific to tight junction formation do not show elevated transcripts in HL-60/S4 cells. Interactions between PVRL2 and MLLT4, between PVRL2 and CD226, as well as PECAM1-PECAM1 and ESAM-ESAM junctions may establish tight junctions between the TPA treated cells, which appear to be unlikely between RA treated HL-60/S4 cells.

Discussion

The present study details the changes in mRNA levels in the HL-60/S4 cell line when differentiated with retinoic acid (RA) or phorbol ester (TPA), leading to granulocyte or macrophage cell forms. The RNA-seq data for each cell state was obtained from quadruplicate independent cell samples yielding measurements of transcript levels with high statistical significance. These data indicated that for both differentiated cell forms, compared with undifferentiated cells, more genes showed increased levels of transcripts than revealed decreased levels. The transcript data was mapped to $\sim 30,000$ isoforms, representing $\sim 16,000$ genes. The examples shown above of phenotypically related gene groups represent a very small sampling of the transcriptomes of undifferentiated, granulocytic and macrophage-differentiated cell forms. As mentioned earlier, we used gene set analysis of KEGG pathways to obtain new insights into processes involved in differentiation. The vast majority of enriched pathways, and all of the most enriched, was common in both treatments. The top 10 most enriched pathways included chemokine, MAPK, B cell, and Toll-like receptor signaling; osteoclast differentiation; lysosome activity; endocytosis; phagocytosis; regulation of actin cytoskeleton; and focal adhesion. Some pathways, such as chemokine signaling, seem to be quite appropriate, since the pathway supports migration, chemotaxis, cell shape change and apoptosis, all attributes of differentiated granulocytes (see Supplemental Figure 1). Others are more surprising, such as osteoclast differentiation (see Supplemental Figure 2). Osteoclasts are multinucleated cells in the monocyte-macrophage lineage. HL-60/S4 TPA-treated macrophage cells are not multinucleated. However, several genes involved in osteoclast differentiation (RANK, DC-STAMP, OC-STAMP and Atp6v0d2)^{44,45} exhibit significantly higher transcript levels after TPA treatment, than after RA treatment (data not shown). Furthermore, the differences in Granule Protein transcripts (described earlier) suggest that the HL-60/S4 macrophage form may be less adapted to fighting bacterial infection, and more adapted to function in bone resorption. Perhaps additional *in vitro* experiments with HL-60/S4 macrophage cells could achieve differentiation into more mature multinuclear osteoclasts. This is one of many examples where analysis of specific pathways suggests new experimental directions.

The current transcriptome analysis details critical genetic data on aspects of nuclear architecture and

chromatin changes occurring during differentiation of HL-60/S4 cells. Ongoing collaborative studies using HL-60/S4 cells are defining RA and TPA induced changes in DNA methylation, nucleosome positioning and occupancy, histone modifications and Hi-C (chromatin proximity). With HL-60/S4 cells now available from ATCC to any laboratory, we anticipate an accelerated understanding of the mechanisms and consequences of cell differentiation within this cell system. To facilitate this progress, we attach a fully searchable data sheet (Supplemental Table 6) containing all of the HL-60/S4 transcriptome data, so that specific transcripts of interest are accessible to the individual researcher. Furthermore, we attach a ranked list of the KEGG enriched pathways for the HL-60/S4 granulocytic and macrophage cell states (Supplemental Table 7). The transcript level changes described in this study of HL-60/S4 cells undergoing granulocytic or macrophage differentiation should reflect changes in mRNA synthesis and degradation. The synthesis changes must arise from structural events occurring at the local chromatin and global nuclear architectural levels. Well characterized and reproducible HL-60/S4 cell differentiation furnishes a convenient model system for additional exploration of these structural events responsible for regulation of differential gene expression.

Addendum

HL-60/S4 Karyotype Analysis We performed 24-color multiplex fluorescence in situ hybridization (M-FISH)⁴⁶ on 2 aliquots of undifferentiated HL-60/S4 cells (one frozen in 2008; the other, in 2012) cultivated under standard conditions with colcemide for 17 h (generally yielding ~40–50% mitotic cells). Following M-FISH, we analyzed images from 15 mitotic spreads of 2008 and 15 from 2012 cells for chromosome number and integrity. The results show that the karyotype of HL-60/S4 cells is abnormal, but stable at the 2 time points with the following ISCN karyotype:

44,X,-X,inv(2),der(3)t(3;14),der(4)t(4;18),der(5)t(5;17;16),der(6)t(6;8;6),der(7)t(5;7),der(9)t(9;14),der(11)t(6;8;11),dup(13),der(14)t(9;14),del(14q),der(15)t(6;16;15),-16,der(16)t(7;16),-17,del(18q),der(21)t(16;21),mar1-2.

A representative example of one mitotic spread from 2008 cells is presented as a multicolor karyogram in Fig. 9. Analyses of all 15 metaphase spreads of the 2008 cells are presented in Supplemental Table 8.

Several general conclusions have emerged from the karyotype analyses: (1) The karyotypes are stable, comparing 2012 and 2008 cell samples. (2) The karyotypes exhibit only one X chromosome and no Y chromosomes. (3) Apparently normal diploid states are observed for chromosomes 1, 8, 10, 12, 19, 20 and 22. (4). Apparently monosomic states are seen for chromosomes 17 and X. (5) Structural aberrations (inversion, duplication, deletions and translocations) involved chromosomes 2, 3, 4, 5, 6, 7, 8, 9, 11, 13, 14, 15, 16, 17, 18 and 21. (6) The karyotype clearly demonstrates the absence of a translocation t(15;17).

The karyotype of the “parent” HL-60 cell line has been examined several times, most recently in 1999, also using M-FISH.⁴⁷ There are both similarities and differences between the parent and derived (HL-60/S4) cell lines. The differences might be attributed to improvements in the M-FISH technique and/or to genetic changes induced during the derivation of HL-60/S4 with the mutagen N-methyl-N'-nitro-N-nitrosoguanidine.¹⁷

There is a considerable amount of transcript data available for normal myeloid cell differentiation⁴⁸ and for acute myeloid leukemia.^{16,49} However, given the massive karyotypic rearrangements of HL-60/S4 cells compared with the normal human karyotype, we suggest that comparisons between HL-60/S4 transcriptomes and those from normal or leukemic myeloid cells should be made with great caution. The reverberations of extensive chromosomal rearrangements upon chromosomal higher order structure, gene proximities and environments could be considerable.

Materials and methods

Cell culture

HL-60/S4 cells were maintained in RPMI 1640 medium, plus 10% fetal calf serum and 1% Pen/Strep(Glutamine. This cell line is newly available from ATCC [www.atcc.org, #CRL-3306]). For the current experiments: undifferentiated HL-60/S4 cells were seeded into 4 separate T-25 flasks (5 ml each at a concentration of 1×10^5); RA (Sigma-Aldrich R2625) treated cells were seeded into 4 separate T-25 flasks (5 ml each at a concentration of 2×10^5 , with RA added to $1 \mu\text{M}$); TPA (Sigma-Aldrich P1585) treated cells were seeded into 4 separate 6 cm diameter petri dishes (5 ml each at a concentration of 4×10^5 , with TPA added to 16 nM). After 4 d, cells were observed and counted: undifferentiated (0), 1.45×10^6 cells/ml; RA treated, 1.48×10^6

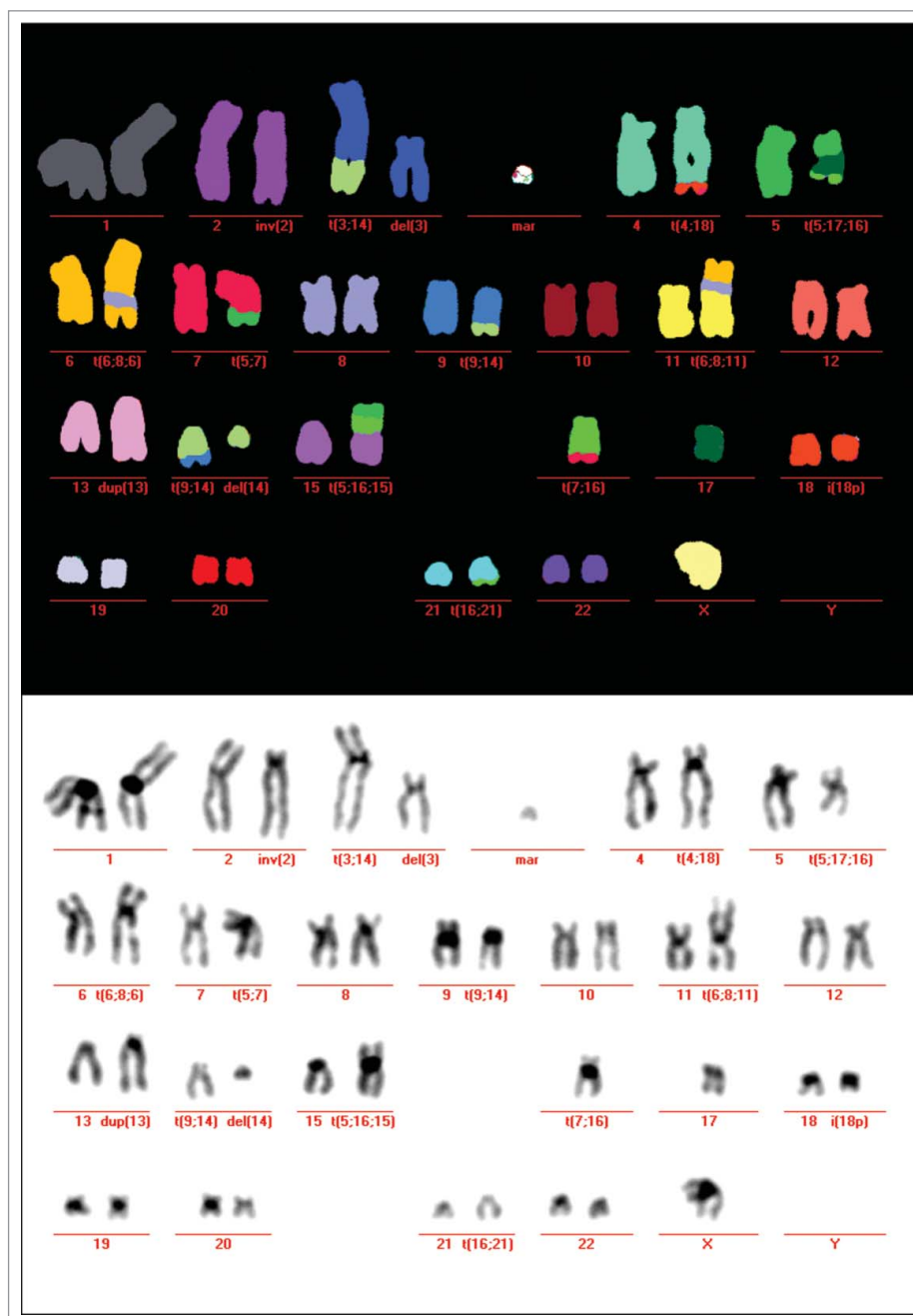


Figure 9. M-FISH Karyotype Analysis of HL-60/S4 Cells. Top, representative multicolor karyogram of undifferentiated HL-60/S4 cells. Each chromosome is presented in a specific classification color allowing the easy detection of numerical and structural chromosome aberrations. Bottom, inverted DAPI staining results in a GTG-like banding pattern of the chromosomes. Data in Supplemental Table 8.

cells/ml; TPA treated, could not be counted due to clumping (see Fig. 5), but based upon previous studies were assumed to be $\sim 5 \times 10^5$ cells/ml.

RNA extraction

Total RNA was isolated using the RNeasy Micro Kit (Qiagen, Hilden, Germany) according to the manufacturer's instructions, with minor modifications. For 0

and RA treated cells, 1.4 ml was harvested from each flask, centrifuged at 420 \times g for 5 min in RNase-free tubes, supernatants removed and 1.4 ml of RLT-buffer containing β -Mercaptoethanol was added. For TPA treated cells, dead cells were decanted from the Petri dish and 1.75 ml RLT-buffer containing β -Mercaptoethanol was added and cells scraped (yielding approximately the same cell concentration as the 0 and RA treated cells). Each of the 4 replicate samples was

individually lysed by vigorous vortexing, immediately frozen in dry ice and stored at -80°C . Subsequently, each thawed lysate was homogenized using QIAshredder spin columns (Qiagen, Hilden, Germany). One volume of 70% EtOH was added, the RNA bound to a RNeasy MinElute spin column and genomic DNA digested by DNase I. Afterwards, DNase I and residual buffer traces were removed by subsequent washing steps and the RNA eluted in $14\ \mu\text{l}$ nuclease-free water (Ambion, ThermoFisher Scientific, Waltham, MA). Integrity and purity of RNA was ensured using a Bioanalyzer 2100 (Agilent, Santa Clara).

RNA library preparation and RNA Sequencing

Library preparation for RNA-sequencing was conducted following the TruSeq RNA Library Preparation Kit v2 (Illumina Inc., San Diego, CA) with minor modifications. In brief, $1\ \mu\text{g}$ of total RNA was fragmented to approx. 150bp and the polyA-RNA fraction reverse transcribed to obtain cDNA. After the end repair, 3' ends were adenylated and the adapters ligated. $10\ \mu\text{l}$ of the ligated adaptor mix was used as PCR template and the number of PCR cycles was limited to 12. The library quality was validated on a DNA Bioanalyzer (Agilent, Santa Clara) and a Qubit fluorometer (ThermoFisher Scientific, Waltham, MA). A PhiX control (1%, #FC-110-3001) was spiked into the resulting library and clustering was done according to the TruSeq PE Cluster Kit v3 (#PE-401-3001, Illumina Inc., San Diego, CA). Sequencing was performed on the HiSeq 2000 platform, which generated 2×100 paired-end reads (TrueSeq SBS Kit v3, #FC-401-3001, Illumina Inc., San Diego).

Determination of differential transcript levels

We followed the RSEM workflow outlined at <http://deweylab.github.io/RSEM> and used the sequences and annotation of UCSC human genome v19 from Illumina igenome (https://support.illumina.com/sequencing/sequencing_software/igenome.html). A bash script of the workflow is available as Supplemental Text 1. Briefly, we used bowtie2 to map paired-end reads to transcripts extracted from the reference genome, and calculated expression values using RSEM v1.2.15. RSEM uses a maximum likelihood expectation-maximization algorithm to estimate the transcript abundance of isoforms from RNA-Seq reads.²⁶ A summary of mapping results is available as

Supplemental Table 9. We then calculated the significance of expression differences using EBSeq v1.1.5 with the ng-vector option for isoform-level analysis.²⁷ We tested RA vs control, TPA vs control, and RA vs TPA, and accepted isoforms with posterior probability greater than or equal to 0.95 as differentially expressed. We used the output of a 3-way test of control vs RA vs TPA to generate the normalized mean count value from the 4 replicates for each condition. See Supplemental Table 6 for a complete table of EBSeq normalized counts and PPDE values for each hg19 transcript. We uploaded lists of differentially expressed genes (HGNC gene symbols) to WebGestalt (<http://bioinfo.vanderbilt.edu/webgestalt>) for gene set enrichment analysis of KEGG pathways.⁵⁰ We considered a KEGG pathway enriched for increased or decreased gene expression if the hypergeometric test returned an adjusted p value less than 0.05. See Supplemental Table 7 for a listing of KEGG pathways enriched in RA- or in TPA-treated cells. Output from RSEM, EBSeq, and WebGestalt were loaded into a MySQL database with hg19 annotation and KEGG data for analysis.

Multiplex fluorescence in situ hybridization

M-FISH was performed, as described.⁵¹ Briefly, 7 pools of flow-sorted human chromosome painting probes were amplified and directly labeled using 7 different fluorochromes (DEAC, FITC, Cy3, Cy3.5, Cy5, Cy5.5 and Cy7) using degenerative oligonucleotide primed PCR (DOP-PCR). Metaphase chromosomes immobilized on glass slides were denatured in 70% formamide/2xSSC pH 7.0 at 72°C for 2 min followed by dehydration in a degraded ethanol series. Hybridization mixture containing combinatorially labeled painting probes, an excess of unlabeled cot1 DNA, 50% formamide, 2xSSC, and 15% dextran sulfate were denatured for 7 min at 75°C , pre-annealed at 37°C for 20 min and hybridized at 37°C to the denatured metaphase preparations. After 48 h the slides were washed in 2xSSC at room temperature for 3×5 min followed by 2 washes in 0.2xSSC/0.2% Tween-20 at 56°C for 7 min, each. Metaphase spreads were counterstained with 4,6-diamidino-2-phenylindole (DAPI) and covered with antifade solution. Metaphase spreads were recorded using a DM RXA epifluorescence microscope (Leica Microsystems, Bensheim, Germany) equipped with a Sensys

CCD camera (Photometrics, Tucson, AZ). Leica Q-FISH software controlled the camera and microscope. Images were processed on the basis of the Leica MCK software and presented as multicolor karyograms (Leica Microsystems Imaging solutions, Cambridge, United Kingdom).

Availability of data and materials

The data sets supporting the conclusions of this article are included within the article, the Additional files and are available in the NCBI Short Read Archive at <http://www.ncbi.nlm.nih.gov/bioproject/303179>

Health and safety

We confirm that all mandatory laboratory health and safety procedures have been complied with in the course of conducting any experimental work reported in this paper.

List of abbreviations

<i>AML</i>	acute myeloblastic leukemia
<i>APL</i>	acute promyelocytic leukemia
<i>DMSO</i>	dimethyl sulfoxide
<i>HGNC</i>	human genome nomenclature committee
<i>INM</i>	inner nuclear membrane
<i>KEGG</i>	Kyoto Encyclopedia of Genes and Genomes
<i>LINC</i>	linker of nucleoskeleton and cytoskeleton
<i>M-FISH</i>	Multiplex fluorescence <i>in situ</i> hybridization
<i>NE</i>	nuclear envelope
<i>RSEM</i>	RNA-Seq by expectation-maximization
<i>RA</i>	retinoic acid
<i>TPA</i>	phorbol ester

Disclosure of potential conflicts of interest

No potential conflicts of interest were disclosed.

Acknowledgments

We thank the High Throughput Sequencing unit of the Genomics & Proteomics Core Facility, German Cancer Research Center (DKFZ), for providing an excellent preparation of the libraries and sequencing services. Verena Thewes (Division of Molecular Genetics, DKFZ) generously performed the RNA extraction and wrote the method description. We thank Brigitte Schoell for excellent technical assistance in chromosome preparation and multicolor FISH experiments. We thank Edward Jachimowicz, Scientific Manager of the Flow Cytometry, Cell Sorting and Cell Analysis Core Facility at Maine Medical Center Research Institute, Scarborough ME for

performing the cell cycle analysis. We thank Jasmine B. Olins (now at Brandeis University, Waltham, MA) and Elizabeth (Lily) Kolle (now at Bowdoin College, Brunswick, ME) for the data in Fig. 5, which was collected in partial fulfillment of their Senior Project at Freeport High School, Freeport, ME.

Funding

DMW thanks the Bay and Paul Foundations for support. ALO and DEO thank the College of Pharmacy at UNE for their support. ALO and DEO were recipients of a 2015 UNE Mini-Grant from the Vice President for Research and Scholarship. ALO and DEO thank the German Cancer Research Center (Heidelberg) for the awards of Guest Scientist fellowships.

Notes on contributors

DMW performed the RNA-Seq analysis, including statistical evaluations and KEGG analyses, and wrote parts of the manuscript. AJ analyzed data (multicolor karyotyping, M-FISH), wrote part of the manuscript, and provided a figure and a table. JL participated in writing, discussions and planning. ALO handled the cellular preparations, wrote parts of the manuscript, prepared some of the figures and participated in discussions and planning. DEO conceived of the project, directed and performed some of the analyses and wrote some of the manuscript. All authors read and approved the final manuscript.

References

- [1] Collins SJ, Gallo RC, Gallagher RE. Continuous growth and differentiation of human myeloid leukaemic cells in suspension culture. *Nature* 1977; 270:347-9; PMID:271272; <http://dx.doi.org/10.1038/270347a0>
- [2] Collins SJ, Ruscetti FW, Gallagher RE, Gallo RC. Terminal differentiation of human promyelocytic leukemia cells induced by dimethyl sulfoxide and other polar compounds. *Proc Natl Acad Sci U S A* 1978; 75:2458-62; PMID:276884; <http://dx.doi.org/10.1073/pnas.75.5.2458>
- [3] Breitman TR, Selonick SE, Collins SJ. Induction of differentiation of the human promyelocytic leukemia cell line (HL-60) by retinoic acid. *Proc Natl Acad Sci U S A* 1980; 77:2936-40; PMID:6930676; <http://dx.doi.org/10.1073/pnas.77.5.2936>
- [4] Dalton WT, Jr., Ahearn MJ, McCredie KB, Freireich EJ, Stass SA, Trujillo JM. HL-60 cell line was derived from a patient with FAB-M2 and not FAB-M3. *Blood* 1988; 71:242-7. PMID:3422031
- [5] Rovera G, Santoli D, Damsky C. Human promyelocytic leukemia cells in culture differentiate into macrophage-like cells when treated with a phorbol diester. *Proc Natl Acad Sci U S A* 1979; 76:2779-83; PMID:288066; <http://dx.doi.org/10.1073/pnas.76.6.2779>
- [6] Rovera G, O'Brien TG, Diamond L. Induction of differentiation in human promyelocytic leukemia cells by

- tumor promoters. *Science* (New York, NY) 1979; 204:868-70; <http://dx.doi.org/10.1126/science.286421>
- [7] Miyaura C, Abe E, Kuribayashi T, Tanaka H, Konno K, Nishii Y, et al. 1 alpha,25-Dihydroxyvitamin D3 induces differentiation of human myeloid leukemia cells. *Biochem Biophys Res Commun* 1981; 102:937-43; PMID:6946774; [http://dx.doi.org/10.1016/0006-291X\(81\)91628-4](http://dx.doi.org/10.1016/0006-291X(81)91628-4)
- [8] Tanaka H, Abe E, Miyaura C, Kuribayashi T, Konno K, Nishii Y, et al. 1 alpha,25-Dihydroxycholecalciferol and a human myeloid leukaemia cell line (HL-60). *Biochem J* 1982; 204:713-9; PMID:6289803; <http://dx.doi.org/10.1042/bj2040713>
- [9] Collins SJ. The HL-60 promyelocytic leukemia cell line: proliferation, differentiation, and cellular oncogene expression. *Blood* 1987; 70:1233-44. PMID:3311197
- [10] Meier RW, Chen T, Mathews S, Niklaus G, Tobler A. The differentiation pathway of HL60 cells is a model system for studying the specific regulation of some myeloid genes. *Cell Growth & Differentiation: the molecular biology journal of the American Association for Cancer Research* 1992; 3:663-9.
- [11] Lee KH, Chang MY, Ahn JI, Yu DH, Jung SS, Choi JH, et al. Differential gene expression in retinoic acid-induced differentiation of acute promyelocytic leukemia cells, NB4 and HL-60 cells. *Biochem Biophys Res Commun* 2002; 296:1125-33; PMID:12207890; [http://dx.doi.org/10.1016/S0006-291X\(02\)02043-0](http://dx.doi.org/10.1016/S0006-291X(02)02043-0)
- [12] Mollinedo F, Lopez-Perez R, Gajate C. Differential gene expression patterns coupled to commitment and acquisition of phenotypic hallmarks during neutrophil differentiation of human leukaemia HL-60 cells. *Gene* 2008; 419:16-26; PMID:18547747; <http://dx.doi.org/10.1016/j.gene.2008.04.015>
- [13] Zheng X, Ravatn R, Lin Y, Shih WC, Rabson A, Strair R, et al. Gene expression of TPA induced differentiation in HL-60 cells by DNA microarray analysis. *Nucleic Acids Res* 2002; 30:4489-99; PMID:12384596; <http://dx.doi.org/10.1093/nar/gkf580>
- [14] Suzuki T, Tazoe H, Taguchi K, Koyama Y, Ichikawa H, Hayakawa S, et al. DNA microarray analysis of changes in gene expression induced by 1,25-dihydroxyvitamin D3 in human promyelocytic leukemia HL-60 cells. *Biomed Res* 2006; 27:99-109; PMID:16847355; <http://dx.doi.org/10.2220/biomedres.27.99>
- [15] Song JH, Kim JM, Kim SH, Kim HJ, Lee JJ, Sung MH, et al. Comparison of the gene expression profiles of monocytic versus granulocytic lineages of HL-60 leukemia cell differentiation by DNA microarray analysis. *Life Sci* 2003; 73:1705-19; PMID:12875902; [http://dx.doi.org/10.1016/S0024-3205\(03\)00515-0](http://dx.doi.org/10.1016/S0024-3205(03)00515-0)
- [16] Wang H, Hu H, Zhang Q, Yang Y, Li Y, Hu Y, et al. Dynamic transcriptomes of human myeloid leukemia cells. *Genomics* 2013; 102:250-6; PMID:23806289; <http://dx.doi.org/10.1016/j.ygeno.2013.06.004>
- [17] Leung MF, Sokoloski JA, Sartorelli AC. Changes in microtubules, microtubule-associated proteins, and intermediate filaments during the differentiation of HL-60 leukemia cells. *Cancer Res* 1992; 52:949-54. PMID:1737356
- [18] Campbell MS, Lovell MA, Gorbosky GJ. Stability of nuclear segments in human neutrophils and evidence against a role for microfilaments or microtubules in their genesis during differentiation of HL60 myelocytes. *J Leukoc Biol* 1995; 58:659-66. PMID:7499963
- [19] Olins AL, Buendia B, Herrmann H, Lichter P, Olins DE. Retinoic acid induction of nuclear envelope-limited chromatin sheets in HL-60. *Exp Cell Res* 1998; 245:91-104; PMID:9828104; <http://dx.doi.org/10.1006/excr.1998.4210>
- [20] Olins AL, Herrmann H, Lichter P, Olins DE. Retinoic acid differentiation of HL-60 cells promotes cytoskeletal polarization. *Exp Cell Res* 2000; 254:130-42; PMID:10623473; <http://dx.doi.org/10.1006/excr.1999.4727>
- [21] Olins AL, Herrmann H, Lichter P, Kratzmeier M, Doenecke D, Olins DE. Nuclear envelope and chromatin compositional differences comparing undifferentiated and retinoic acid- and phorbol ester-treated HL-60 cells. *Exp Cell Res* 2001; 268:115-27; PMID:11478838; <http://dx.doi.org/10.1006/excr.2001.5269>
- [22] Olins AL, Hoang TV, Zwerger M, Herrmann H, Zentgraf H, Noegel AA, et al. The LINC-less granulocyte nucleus. *Eur J Cell Biol* 2009; 88:203-14; PMID:19019491; <http://dx.doi.org/10.1016/j.ejcb.2008.10.001>
- [23] Olins AL, Ernst A, Zwerger M, Herrmann H, Olins DE. An in vitro model for Pelger-Huet anomaly: stable knockdown of lamin B receptor in HL-60 cells. *Nucleus* 2010; 1:506-12. PMID:21327094
- [24] Rowat AC, Jaalouk DE, Zwerger M, Ung WL, Eydelnant IA, Olins DE, et al. Nuclear envelope composition determines the ability of neutrophil-type cells to passage through micron-scale constrictions. *J Biol Chem* 2013; 288:8610-8; PMID:23355469; <http://dx.doi.org/10.1074/jbc.M112.441535>
- [25] Olins AL, Ishaque N, Chotewutmontri S, Langowski J, Olins DE. Retrotransposon Alu is enriched in the epichromatin of HL-60 cells. *Nucleus* 2014; 5:237-46. PMID:24824428
- [26] Li B, Dewey CN. RSEM: accurate transcript quantification from RNA-Seq data with or without a reference genome. *BMC bioinformatics* 2011; 12:323; PMID:21816040; <http://dx.doi.org/10.1186/1471-2105-12-323>
- [27] Leng N, Dawson JA, Thomson JA, Ruotti V, Rissman AI, Smits BM, et al. EBSeq: an empirical Bayes hierarchical model for inference in RNA-seq experiments. *Bioinformatics* 2013; 29:1035-43; PMID:23428641; <http://dx.doi.org/10.1093/bioinformatics/btt087>
- [28] Borregaard N, Sorensen OE, Theilgaard-Monch K. Neutrophil granules: a library of innate immunity proteins. *Trends Immunol* 2007; 28:340-5; PMID:17627888; <http://dx.doi.org/10.1016/j.it.2007.06.002>
- [29] Soehnlein O, Weber C, Lindbom L. Neutrophil granule proteins tune monocytic cell function. *Trends Immunol* 2009; 30:538-46; PMID:19699683; <http://dx.doi.org/10.1016/j.it.2009.06.006>

- [30] Pass MB, Borregaard N, Cowland JB. Derangement of transcription factor profiles during in vitro differentiation of HL60 and NB4 cells. *Leuk Res* 2007; 31:827-37; PMID:16942795; <http://dx.doi.org/10.1016/j.leukres.2006.07.019>
- [31] Olins AL, Olins DE. Cytoskeletal influences on nuclear shape in granulocytic HL-60 cells. *BMC Cell Biol* 2004; 5:30; PMID:15317658; <http://dx.doi.org/10.1186/1471-2121-5-30>
- [32] Olins AL, Rhodes G, Welch DB, Zwerger M, Olins DE. Lamin B receptor: multi-tasking at the nuclear envelope. *Nucleus* 2010; 1:53-70. PMID:21327105
- [33] Mejat A, Misteli T. LINC complexes in health and disease. *Nucleus* 2010; 1:40-52. PMID:21327104
- [34] Tapley EC, Starr DA. Connecting the nucleus to the cytoskeleton by SUN-KASH bridges across the nuclear envelope. *Curr Opin Cell Biol* 2013; 25:57-62; PMID:23149102; <http://dx.doi.org/10.1016/j.ceb.2012.10.014>
- [35] Asghar U, Witkiewicz AK, Turner NC, Knudsen ES. The history and future of targeting cyclin-dependent kinases in cancer therapy. *Nat Rev Drug Discovery* 2015; 14:130-46; PMID:25633797; <http://dx.doi.org/10.1038/nrd4504>
- [36] Lim S, Kaldis P. Cdks, cyclins and CKIs: roles beyond cell cycle regulation. *Development* 2013; 140:3079-93; PMID:23861057; <http://dx.doi.org/10.1242/dev.091744>
- [37] Ochsenreither S, Majeti R, Schmitt T, Stirewalt D, Keilholz U, Loeb KR, et al. Cyclin-A1 represents a new immunogenic targetable antigen expressed in acute myeloid leukemia stem cells with characteristics of a cancer-testis antigen. *Blood* 2012; 119:5492-501; PMID:22529286; <http://dx.doi.org/10.1182/blood-2011-07-365890>
- [38] Cho JW, Jeong YW, Kim KS, Oh JY, Park JC, Lee JC, et al. p21(WAF1) is associated with CDK2 and CDK4 protein during HL-60 cell differentiation by TPA treatment. *Cell Proliferation* 2001; 34:267-74; PMID:11591175; <http://dx.doi.org/10.1046/j.0960-7722.2001.00208.x>
- [39] Rossetto D, Avvakumov N, Cote J. Histone phosphorylation: a chromatin modification involved in diverse nuclear events. *Epigenetics* 2012; 7:1098-108; PMID:22948226; <http://dx.doi.org/10.4161/epi.21975>
- [40] Martin SJ, Bradley JG, Cotter TG. HL-60 cells induced to differentiate towards neutrophils subsequently die via apoptosis. *Clin Exp Immunol* 1990; 79:448-53; PMID:2317949; <http://dx.doi.org/10.1111/j.1365-2249.1990.tb08110.x>
- [41] Watson RW, Rotstein OD, Parodo J, Bitar R, Hackam D, Marshall JC. Granulocytic differentiation of HL-60 cells results in spontaneous apoptosis mediated by increased caspase expression. *FEBS Lett* 1997; 412:603-9; PMID:9276475; [http://dx.doi.org/10.1016/S0014-5793\(97\)00779-5](http://dx.doi.org/10.1016/S0014-5793(97)00779-5)
- [42] Solary E, Bertrand R, Pommier Y. Apoptosis of human leukemic HL-60 cells induced to differentiate by phorbol ester treatment. *Leukemia* 1994; 8:792-7. PMID:8182936
- [43] Sonoda Y, Matsumoto Y, Funakoshi M, Yamamoto D, Hanks SK, Kasahara T. Anti-apoptotic role of focal adhesion kinase (FAK). Induction of inhibitor-of-apoptosis proteins and apoptosis suppression by the overexpression of FAK in a human leukemic cell line, HL-60. *J Biol Chem* 2000; 275:16309-15; PMID:10821872; <http://dx.doi.org/10.1074/jbc.275.21.16309>
- [44] Wada T, Nakashima T, Hiroshi N, Penninger JM. RANKL-RANK signaling in osteoclastogenesis and bone disease. *Trends Mol Med* 2006; 12:17-25; PMID:16356770; <http://dx.doi.org/10.1016/j.molmed.2005.11.007>
- [45] Zhang C, Dou CE, Xu J, Dong S. DC-STAMP, the key fusion-mediating molecule in osteoclastogenesis. *J Cellular Physiol* 2014; 229:1330-5; PMID:24420845; <http://dx.doi.org/10.1002/jcp.24553>
- [46] Speicher MR, Gwyn Ballard S, Ward DC. Karyotyping human chromosomes by combinatorial multi-fluor FISH. *Nat Genet* 1996; 12:368-75; PMID:8630489; <http://dx.doi.org/10.1038/ng0496-368>
- [47] Liang JC, Ning Y, Wang RY, Padilla-Nash HM, Schrock E, Soenksen D, et al. Spectral karyotypic study of the HL-60 cell line: detection of complex rearrangements involving chromosomes 5, 7, and 16 and delineation of critical region of deletion on 5q31.1. *Cancer Genet Cytogenetics* 1999; 113:105-9; PMID:10484974; [http://dx.doi.org/10.1016/S0165-4608\(99\)00030-8](http://dx.doi.org/10.1016/S0165-4608(99)00030-8)
- [48] Schonheit J, Leutz A, Rosenbauer F. Chromatin dynamics during differentiation of myeloid cells. *J Mol Biol* 2015; 427:670-87; PMID:25172539; <http://dx.doi.org/10.1016/j.jmb.2014.08.015>
- [49] Ilyas AM, Ahmad S, Faheem M, Naseer MI, Kumosani TA, Al-Qahtani MH, et al. Next generation sequencing of acute myeloid leukemia: influencing prognosis. *BMC Genomics* 2015; 16 Suppl 1:S5; PMID:25924101; <http://dx.doi.org/10.1186/1471-2164-16-S1-S5>
- [50] Zhang B, Kirov S, Snoddy J. WebGestalt: an integrated system for exploring gene sets in various biological contexts. *Nucleic Acids Res* 2005; 33:W741-8; PMID:15980575; <http://dx.doi.org/10.1093/nar/gki475>
- [51] Geigl JB, Uhrig S, Speicher MR. Multiplex-fluorescence in situ hybridization for chromosome karyotyping. *Nat Protoc* 2006; 1:1172-84; PMID:17406400; <http://dx.doi.org/10.1038/nprot.2006.160>